AN INVESTIGATION OF THE VARIATION OF PORE STRUCTURE IN EUCALYPTUS FIBRE DURING RECYCLING

Wen-Jie Guo,[a] Yan Wang,[a] Ming-Zhi Huang,[a] Jin-Quan Wan,[b,*] and Yong-Wen Ma [a]

Variation in the pore structure of eucalyptus fibre during recycling was investigated using low-temperature nitrogen adsorption, atomic force microscopy (AFM), and fractal geometry. The Brunauer-Emmett-Teller (BET) surface area of the fibre fell to 55.1% of the original value after the first cycle, and to 49.0% after the second cycle, ultimately declining to 35.0% after the fourth. The Barret-Joyner-Halenda (BJH) adsorption cumulative pore volume fell to 38.4% of the original by the fourth. After four cycles, the average pore diameter fell to 82% of the original. AFM tests showed that the pore structure in fibre expressed high self-similarity in statistics, and the pore structure in the fibre could be regarded as a fractal. Fractal geometry analysis of the results showed that the fractal dimension of eucalyptus virgin fibre is 2.954. With the number of process cycles increasing, the fractal dimension fell to a minimum of 2.886 after four cycles. The water retention value (*WRV*) of the fibre was proportional to the fractal dimension and the crystallinity of fibre.

Keywords: Pore structure; Fractal; Low-temperature nitrogen adsorption; AFM; Eucalyptus fibre

*Contact information: a: School of Environmental Science and Engineering, South China University of Technology, Guangzhou 510006, China; b: State Key Laboratory of Pulp and Paper Engineering, South China University of Technology, Guangzhou 510641, China; * Corresponding author: ppjqwan@scut.edu.cn*

INTRODUCTION

Plant fibres used for papermaking are porous materials. Pores are a natural feature of native wood fibres, but additional pores are created during the pulping and bleaching processes when lignin and hemicellulose are removed from the wood cell wall (Maloney and Paulapuro 1999; Topgaard and Soderman 2002). Pore size and pore size distributions in the fibre walls are also influenced by mechanical and chemical treatments such as beating, drying, and the use of wet strength agents (Häggkvist et al. 1998). The cell wall pore structure plays a significant role in determining fibre properties, such as the capacity for fibre swelling, the strength of paper, etc. (Andreasson et al. 2003; Maloney and Paulapuro 1999). The characterization of pore size and pore size distribution is important for the understanding of fibre properties. Different methods can be used to characterize the cell wall pores. The most frequently used method is the solute exclusion technique (Böttger et al. 1983). Other techniques, such as inverse size exclusion chromatography (Berthold and Salmén 1997), the NMR relaxation method (Häggkvist 1998) and low-temperature nitrogen adsorption (Chen et al. 2009; Mancosky et al. 2004; Yu et al. 2009) are also available.

However, pore geometry is not easily described. Pore size, shape, surface area, and connectivity all exhibit varying levels of complexity. Simplification of structure has traditionally been used to enable these geometric problems to be described in "Euclidean" terms, but the inadequacies of this approach are well known. There is strong interest

surrounding the possibility of better describing these natural geometric structures which are often irregular, jagged, or fragmented. Modern geometry is now able to sum up the complexity of real objects and has brought into analytical consideration forms (Atzeni et al. 2008). One of the new conceptual instruments at the disposition of researchers is "Fractal Geometry", which was developed during the last century but which is especially linked to its recognition and formalization in the 1970s by Mandelbrot (1982).

Fractal geometry allows the characterization of objects in terms of their self-similar (scale invariant) properties, i.e., parts of the object are similar to the whole after rescaling (Mandelbrot 1982). Fractal techniques have been used in diverse engineering applications that involve physical phenomena in disordered structures and over multiple scales (Pitchumani and Ramakrishnan 1999). In all of these applications the fractal dimensions have been very effective in making complex structures easy for analysis, and it is this capability that inspires the current study to perform fractal analysis on pore structures. There have been many studies concerning pore structure related to fractal geometry (Avnir et al. 1983; Farin and Avnir 1988; Pfeifer and Avnir 1983). Most surfaces are fractal in nature within a limited size scale; i.e., they are characteristically self-similar upon the variation of measuring resolution. Fractal dimensions, that describes such fractal materials, were found to be in the complete range $2 < D < 3$: low D values indicate regularity and smoothness, intermediate D values indicate irregular surfaces, and D values close to 3 indicate highly irregular surface (Dobrescua et al. 2003). As for the fractal analysis of porous pulp fibres, little research has been done. It is therefore necessary to develop a new fractal model for porous pulp fibres.

In this study, low-temperature nitrogen adsorption measurements were performed to investigate possible differences in the pore size and pore size distribution of fibre samples during recycling. Atomic force microscopy (AFM) was used to survey the surface topography of eucalyptus virgin pulp fibre. Using the fractal geometry, the fractal dimensions of fibre samples were calculated to quantitatively describe the pore structure in the fibre samples. The relation between fractal dimension and water retention value (*WRV*) was also investigated.

EXPERIMENTAL

Materials

Eucalyptus wood chips were cooked in autoclaves according to the conventional kraft process. Eucalyptus was cooked at a liquor-to-wood ratio of 4.5 and the effective alkali was 5 mol/kg and the sulphidity was 30%. The temperature was raised from 80 to 170℃ at 1 ^{o}C/min and kept at 170 ^{o}C for 180 min. The kappa number of sample was determined to be 76 (after 30 min of cooking), 58 (45 min), 25 (105 min), 23 (120 min), and 18 (180 min).

The kappa-number test was a standardized indirect method for determining the lignin content of pulps (ISO 302 standard). The viscosity was determined according to the ISO 5351/1 standard and brightness from split sheet surface ISO 2470. The total residual lignin content (TRLC) was evaluated from the kappa number according to TRLC / (kappa number) / 6.546 (Gustafsson et al. 2003).

Paper Recycling

Repetitive cycles of treatment were carried out on a Rapid-Köthen sheet former (PK3, PTI laboratory equipment Co, Austria), under constant conditions of 90 °C, -0.94 bar, and 10 min drying time to produce paper sheets with a grammage of 80 g/m^2. From each cycle, some sheets were tested for analysis, and the remainder were soaked in deionized water for at least 12 hours. The re-wetted paper sheets were then disintegrated for 30,000 revolutions in a disintegrator. The recycled pulp was then made into paper sheets and dried. The recycling procedure was repeated for a total of four cycles.

Water Retention Values (*WRV*) Measurements

The pulp or paper was immersed in deionized water for 24 hours, and then centrifuged at 3000 rev/min for 15 minutes at room temperature. Finally, the samples were dried to constant weight at 105°C. From the weights of the wet and dry pulps and, *WRV* was calculated as follows:

$$WRV = \frac{m_0 - m_1}{m_1} \times 100\% \quad (1)$$

where m_0 is the wet pulp mass and m_1 is the dry pulp mass.

Low-Temperature Nitrogen Adsorption Measurements

Wet fibre dehydration is a particularly important process relative to the pore structure of fibres, which contain a large proportion of water. Several methods have been proposed in the technology fibre dehydration, and among them, vacuum freeze-drying is one of the most advanced dehydration methods, providing a dry production, with porous structure and little or no shrinkage (Pachulski and Ulrich 2007; Wang et al. 2007). All samples were freeze dried at -81.8 °C and 760 torr for 8 hours using a vacuum freeze drier (4KBTXL-75, Virtis Co., USA) to remove residual water from fibres. The low-temperature nitrogen adsorption measurements were carried out using an ASAP 2020M micropore analyzer (Micromeritics Co., USA). High-purity N_2 was used as adsorbate, and the absorption-desorption of high-purity N_2 was determined at 77 K with a liquid nitrogen trap using a static volumetric method. The manufacturer's software provides values for the Brunauer-Emmett-Teller (BET) surface area, sizes of macropores, mesopores and micropores, total pore volume, and average pore size of porous materials by applying the BET equation, Barret-Joyner-Halenda (BHJ) mode, Horvath-Kawazoe (H-K) mode, DFT (Density functional theory), and T-plot to the adsorption data (Passe-Coutrin et al. 2008; Sing 2001).

AFM Measurements

Analysis of the pulp or fibre was carried out with a Multimode SPM microscope (Veeco Instruments Inc., USA) in tapping mode. The pulp was diluted in deionized water, dispersed adequately, then the pulp suspension was dropped on a glass slide. The samples were freeze-dried at -81.8 °C and 760 torr for 8 hours using a vacuum freeze drier (4KBTXL-75, Virtis Co., USA) to remove residual water from fibres. The samples were scanning in an atmospheric environment, with scanning frequency of 1.0 to 1.5 Hz and voltage of 600 to 800 mV.

RESULTS AND DISCUSSION

Low-Temperature Nitrogen Adsorption Results

The characterization of BET surface area, pore volume, pore sizes, and pore size distributions is important for understanding fibre properties such as swelling ability and flexibility (Maloney and Paulapuro 1999). In this study, low-temperature nitrogen adsorption method was used to investigate possible differences in the pore size and pore size distribution of fibre samples during recycling. The results of the low-temperature nitrogen adsorption measurements are given in Tables 1 and 2.

Table 1. Pore Data for Eucalyptus Pulp Fibre

Type of pulp	BET surface area, $m^2 \cdot g^{-1}$	BJH adsorption cumulative volume of pores, $cm^3 \cdot g^{-1}$	BJH adsorption average pore diameter, nm
Virgin pulp	31.90	0.0354	5.0
First cycle	17.59	0.0224	4.5
2nd cycle	15.63	0.0176	4.5
Third cycle	12.33	0.0145	4.2
Fourth cycle	11.17	0.0136	4.1

Table 1 shows that recycling had an impact on the BET surface area of the fibre. The BET surface area of the fibre fell to 55.1% of the original value after one cycle, and to 49.0% after two cycles, finally declining to 35.0% of the original value after four cycles. This change is mainly attributable to irreversble pore closure, causing the internal fibre volume to shrink during recycling. With increasing number of cycles, the phenomenon progresses unceasingly. Accordingly, the BET surface area of the fibre decreases monotonically with increasing number of cycles. Continued recycling had an influence on the BJH adsorption cumulative volume of pores of the fibre. With increasing numbers of cycles, the BJH adsorption cumulative volume of pores decreased to 63.3% after one cycle, and then rapidly declined to 38.4% after four cycles. With increasing number of cycles, the pore in fibre is compressed, even closed, this leads to the decrease of the pore volume of fibre.

The average pore size of the virgin pulp fibre, measured by low-temperature nitrogen adsorption, was 5.0 nm. This basically agrees with previous research. For example, Li and Eriksson (1994) found that the average pore size of unbleached wood pulp was 9 to 11 nm (obtained by NMR), and Stone and Scallan (1965) obtained the average pore sizes for different yield wood pulps as 1.2-6 nm (based on size-exclusion chromatography). The recycling had an impact on the BJH adsorption average pore diameter. With increasing number of cycles, the BJH adsorption average pore diameter fell to 90.0% after one cycle, and declined to 82.0% after four cycles. The varying of the pore volume in fibres is related to the transformation among micropores, mecropores, and macropores.

The pore size distributions of the eucalyptus pulp fibres are shown in Table 2.

Table 2. Pore Distributions of Eucalyptus Pulp Fibres

Pore size range, nm	BJH adsorption incremental pore volume, $cm^3 \cdot g^{-1}$				
	Virgin pulp	First-cycle pulp	Second-cycle pulp	Third-cycle pulp	Fourth-cycle pulp
475.2-201.2	0.000493	0.000554	0.000441	0.000773	0.000535
201.2-96.2	0.000387	0.000599	0.000533	0.000726	0.000481
96.2-77.1	0.000123	0.000299	0.000337	0.000231	0.000286
77.1-40.0	0.000755	0.000838	0.000759	0.000646	0.000717
40.0-27.1	0.000651	0.000593	0.000540	0.000617	0.000411
27.1-20.6	0.000623	0.000587	0.000526	0.000164	0.000295
20.6-16.6	0.000595	0.000575	0.000476	0.000816	0.000395
16.6-13.9	0.000576	0.000525	0.000480	0.000393	0.000370
13.9-11.7	0.000770	0.000532	0.000459	0.000584	0.000540
11.7-10.5	0.000596	0.000427	0.000273	0.000444	0.000191
10.5-8.4	0.001420	0.000963	0.000703	0.000931	0.000415
8.4-7.0	0.001544	0.000938	0.000612	0.000849	0.000586
7.0-6.0	0.001621	0.000946	0.000662	0.000845	0.000588
6.0-5.2	0.001718	0.000933	0.000639	0.000517	0.000602
5.2-4.1	0.003948	0.001941	0.001136	0.001084	0.001017
4.1-3.0	0.006526	0.003696	0.002641	0.001248	0.001973
3.0-2.0	0.011800	0.006696	0.009393	0.002853	0.003863
2.0-1.9	0.001225	0.000751	0.000907	0.000793	0.000320

From Tables 1 and 2, it can be seen that the pore size distribution in the eucalyptus pulp fibres was between 1.9 and 500 nm, and there were mainly mesopores and a small amount of micropores and macropores. The volumes of the micropores, mesopores, and macropores of virgin pulp fibre were 0.0012, 0.0328, and 0.0014 $cm^3 \cdot g^{-1}$, respectively. After first-recycling, the volumes of the micropores, mesopores, and macropores of the fibre dropped to 0.0019, 0.0198, and 0.0007 $cm^3 \cdot g^{-1}$, respectively. After third-recycling, the volumes of the micropores, mesopores, and macropores of the fibre dropped to 0.0020, 0.0117, and 0.0008 $cm^3 \cdot g^{-1}$, respectively. With increasing number of cycles, the volumes of the mesopores of the fibre and its percentage decreased, but the percentage of the masopores volumes of the fibre increased, the percentage of the

micropores volumes of the fibre changed little; after third-recycling, they all tended to stabilize.

The physical properties and chemical components of pulp fibres will change after each recycling. The change in the chemical composition can affect the pore structure (Andreasson et al. 2003). The pentosans content of pulp fibres decreased after recycling. The decrease in pentosans is mainly due to the decrease in strong hydrophilic low-molecular weight pentosans (Shao 2001). The dissolution of the hydrophilic low-molecular weight pentosans can cause the surface of fibres to crack and even to rupture, and accordingly, the pore structure of fibres is changed. The drying and pressing processes can also affect the fibre pore structure during recycling (Diniz et al. 2004). The drying and pressing are aimed at fibre dewatering. During drying and pressing, fibre dewatering produces many irreversible changes. For example, there can be fibre cell decomposition, crushing, and irreversible change of pore sizes (Chen et al. 2009).

Atomic Force Microscopy (AFM) Survey

AFM can be used to examine the surface topography of fibre. Fahlén and Salmén (2003) used AFM to obtain more information about the arrangement of cellulose aggregates (fibrils) in the secondary cell wall layer of spruce wood. Notley and Wågberg (2005) examined the model cellulose II surfaces with different surface charge by means of AFM. Kontturi and Vuorinen (2009) characterized the dimension of the resulting cellulose nanocrystals by means of AFM; the fibers came from the dried, and the never-dried chemical pulps were subjected to strong sulfuric acid hydrolysis.

This study used AFM to examine the surface topography of eucalyptus virgin pulp fibre, as shown Fig. 1. In these pictures, the shade expresses different altitude of the fibre surface. When the color is lighter, this implies greater height. So the dark regions in these pictures express the pores and gaps in the fibre. As shown in Fig. 1, there were many pores in the fibre surface, the pore size varied remarkably. Also, as can be seen, along with the decrease of scanning range and the increase of the scanning resolution, all pictures tended to resemble each other. In other words, the pore structure in the fibre expressed high self-similarity in statistics. Therefore, the pore structure in fibre can be regard as a fractal and analyzed by fractal theory.

Fractal Characteristics of the Pores in Cellulose Fibres

Fractal geometry (Liu 2006), describes figures whose segments are similar to their complete form. The radical characteristics of a fractal figure are self-comparability and scale-invariance. Self-comparability means that certain configurations or processes are always similar to each other at all scales or times. In other words, its part and whole properties are similar. The physical essence of this self-comparability is scale-invariance. It is this scale-invariance that means the observer can zoom in on any part in a fractal figure, and the enlarged figure will be similar to the source. So when zooming in or out of a fractal figure, its morphology, complexity and irregularity do not change. Fractals are grouped into regular fractals and irregular fractals. Regular fractals have strict self-comparability, whereas irregular fractals have only statistical self-comparability. The fractal dimension, D, is the parameter which represents the characteristic of a fractal structure.

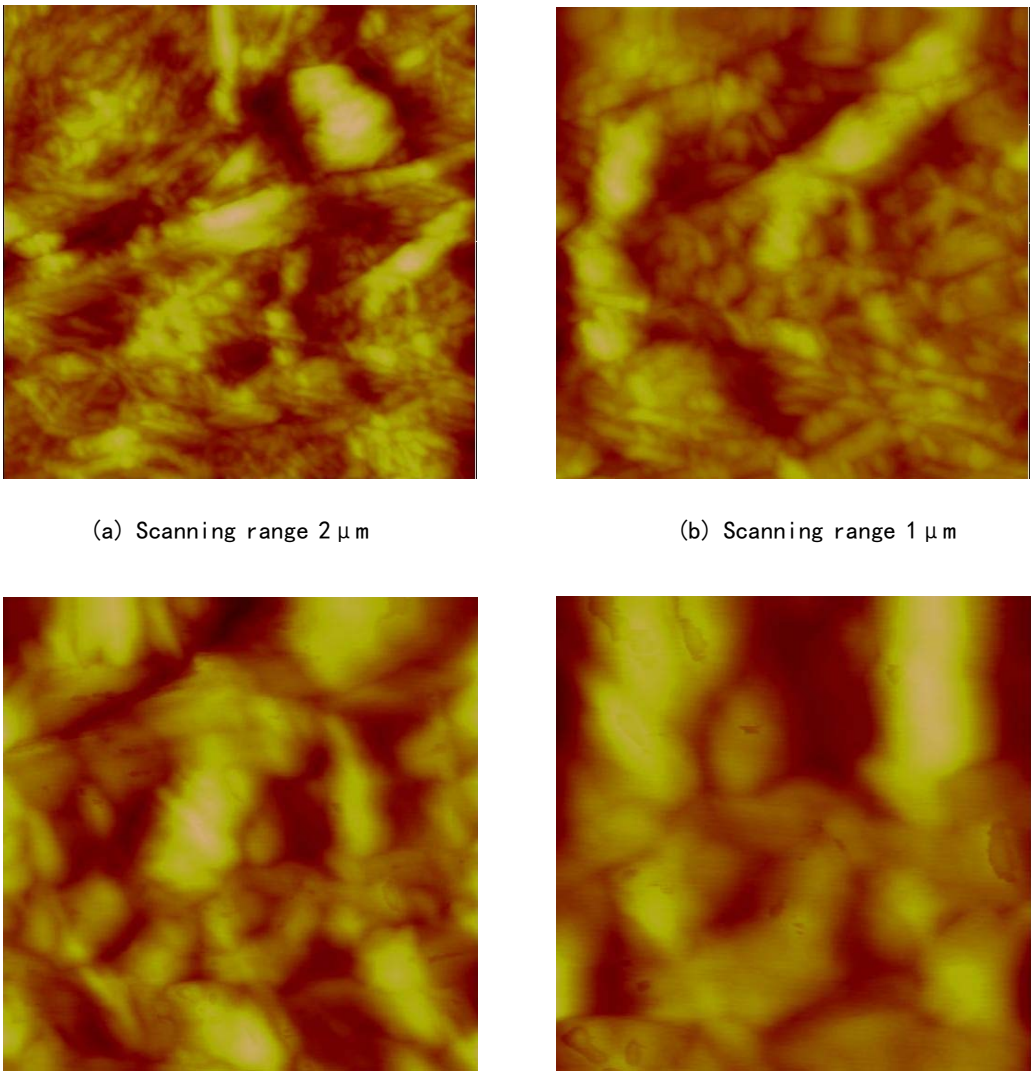

Fig.1. Surface topography of eucalyptus pulp fiber

Self-comparability can be described in mathematically as follows,
For all values of λ>0, if

$$F(\lambda x) = \lambda^{D} F(x) \quad (2)$$

then the figure is self-comparable, where *D* is a constant, namely the fractal dimension.

Katz and Thompson (1985) analyzed the geometric structure of pore materials. Their study showed that both the pore spaces and surfaces were fractal, and that their fractal dimensions were equal. The fractal dimension could be applied to forecast the void fraction of a pore material. Friesen and Mikula (1987) also showed that a pore material was fractal if its pore size was in the range of 1 nm to 1 μm, and the roughness and complexity of the fractal dimension of a pore material could be quantified (Coppens

and Froment 1995; Friesen and Mikula 1987; Leon 1998). If the fractal dimension of a pore material is between 2 and 3, the larger the value of *D* is, the more complex the pore structure is.

The majority of actual figures do not exhibit strict self-comparability, and are hence irregular fractals. Such figures may, however, exhibit self-comparability in certain ranges. Yu (2003) has also given a criterion which decided whether a porous material was fractal, namely,

$$\left(\frac{\lambda_{\min}}{\lambda_{\max}}\right)^{D_f} = 0 \tag{3}$$

where $\lambda_{\min}$ and $\lambda_{\max}$ were the minimum and maximum values of the pore size of a porous material, while D_f was the fractal dimension of the material. Meanwhile, D_f was between 2 and 3 to three-dimensional space.

From a fractal geometry based interpretation of the pore structure of a fibre, the pore size, *r*, and the number of pores, *N (> r),* of size greater *r,* has the following relationship,

$$N(>r) = \int_r^{r_{\max}} f(r)dr = k_0 r^{-D} \tag{4}$$

where r_{max} is the largest pore size in a fibre, $f(r)$ is the pore size function, k_0 is a constant, and *D* is the fractal dimension of a fibre.

Equation (4) may be written as,

$$f(r) = \frac{dN(>r)}{dr} = k_1 r^{-1-D} \tag{5}$$

where k_1 is a constant, which equals $-Dk_0$.

The cumulative volume *V(<r)* of pores sized less than *r,* can be written:

$$V(<r) = \int_{r_{\min}}^{r} f(r)cr^3 dr \tag{6}$$

From Eqs. (5) and (6) the cumulative volume *V(<r)* of pores sized less than *r,* can be rewritten as,

$$V(<r) = k_2\left(r^{3-D} - r_{\min}^{3-D}\right) \tag{7}$$

where k_2 is a constant, which equals $ck_1/(3-D)$.

In the same way, the overall pore volume of a fibre is

$$V = k_2\left(r_{\max}{}^{3-D} - r_{\min}^{3-D}\right) \tag{8}$$

where *S* is the cumulative volume fraction with pore size less than *r*, and *S* can be given by

$$S = \frac{V(r)}{V} = \frac{r^{3-D} - r_{\min}^{3-D}}{r_{\max}^{3-D} - r_{\min}^{3-D}} \tag{9}$$

Considering $r_{min} << r_{max}$, Eq. (9) can be rewritten as

$$S = \left(\frac{r}{r_{\max}}\right)^{3-D} \tag{10}$$

$$\ln S = (3-D)\ln r + K \tag{11}$$

where K is a constant that equals $-(3-D)\ln r_{\max}$.

As for pulp fibre, it is a porous material having a pore size between 1 nm and 500 nm, and $r_{\min}/r_{\max}$ is very small, approximately equal to 0.01; therefore we can approximatively regard $(r_{min} / r_{max})^{Df}$ as zero. We can determine the relation between the pore volume and the pore size of pulp fibre by means of certain method, calculate ln*S*, and then draw out the curve of ln*S* versus ln*r*. If the curve is linear, the slope of the curve is 3-*D*, and *D* is between 2 and 3; this indicates the pore structure of pulp fibre meets scale-invariance, so we can regard the pore structure of pulp fibre as a being fractal, and *D* is the fractal dimension of the pulp fibre.

From Table 2, *S* is calculated; allowing the curves of ln*S* versus ln*r* shown in Figs. 2 to 6 to be plotted.

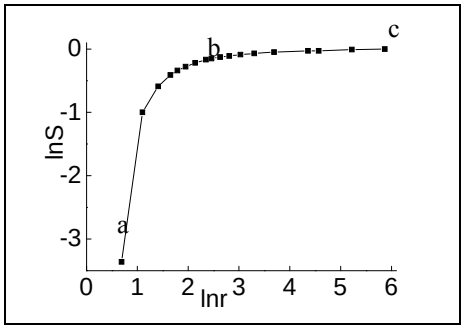

Fig. 2. ln*S* versus ln*r* (virgin pulp fibre)

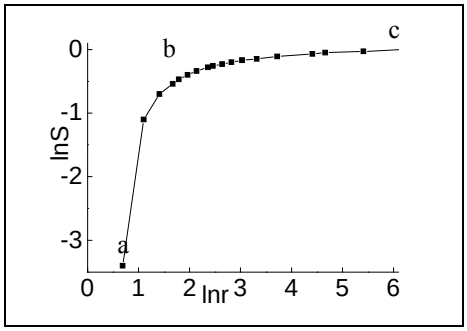

Fig. 3. ln*S* versus ln*r* (first-recycle pulp)

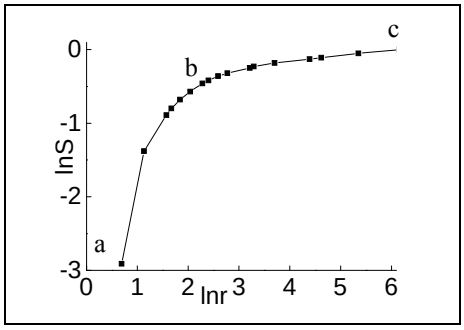

Fig. 4. ln*S* versus ln*r* (second-recycle pulp)

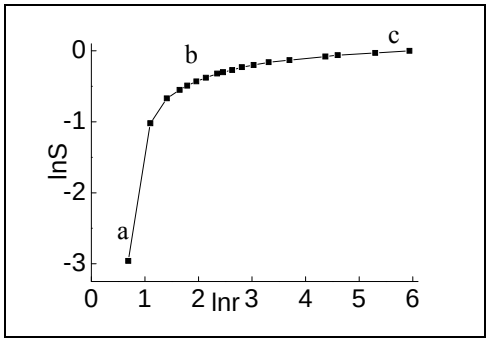

Fig. 5. ln*S* versus ln*r* (third-recycle pulp fibre)

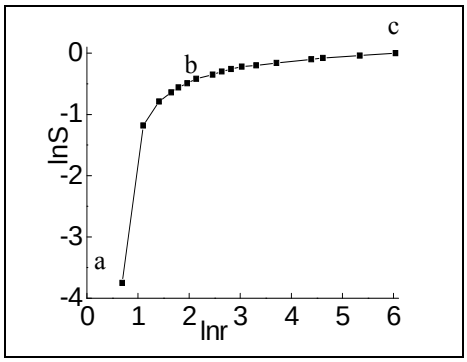

Fig. 6. ln*S* versus ln*r* (fourth-recycle pulp fibre)

From Figs. 2 to 6, it can be seen that the curves of ln*S* versus ln*r* are partly linear. These segments are marked *bc*, corresponding to a pore size of approximately 10 nm to 500 nm. Therefore, we can regard a fibre as a fractal figure in this range. In the smaller pore size range, marked as segment *ab*, with a pore size less than 10nm, there is noticeable negative deviation. This is mainly because the resolution of micropore analyzer is approximately 1.9 nm, so the fine pores are not fully resolved. It is also possible that residual moisture in the cellulose fibre has some effect.

From Figs. 2 to 7 and Equation (11), the fractal dimensions *D* of the recycled fibres can be calculated, as shown in Table 3.

The fractal dimension quantifies the irregularity of a porous material. The fractal dimension *D* of a rough surface is between 2 to 3; the smaller the value of *D* is, the less irregular the surface is.

As shown in Table 3, with increasing numbers of cycles, *D* continuously decreased, finally declining to 97.70% of the original value after four cycles. The declining value of *D* after four cycles indicated that the pulp was smoother than the virgin pulp. Pores exist already in native wood fibres but are also created during the pulping and bleaching processes when lignin and hemicellulose are removed from the wood cell wall. The pore sizes and the pore size distributions in the fibre walls are also influenced by mechanical and chemical treatments such as beating, drying, and the use of wet strength agents. As the number of cycles increased, and the fibre experienced more drying and pressing, the fibre pore tended to become gradually more uniform (Andreasson et al. 2003; Forsstrom et al. 2005; Weise and Paulapuro 1996), indicated by the continuing decline of the fractal dimension. After four cycles, further drying and pressing had little impact on pore structure, which can be perceived as a minimum fractal dimension value.

Table 3. *D* and *WRV* Data of Recycled Eucalyptus Pulp Fibre

Type of pulp	*D*	*WRV*, %
virgin	2.954	151
first-cycle	2.928	131
second-cycle	2.911	120
third-cycle	2.908	115
fourth-cycle	2.886	109

The Relation of the Fractal Dimension of the Cellulose Fibre to *WRV*

The fractal dimension of a cellulose fibre has an important impact on *WRV*. The relationship between *D* and *WRV* is shown in Table 3.

The fibre *WRV* is proportional to the degree of fibre swelling, and this fibre swelling is responsible for the development of binding force between the fibres when paper is dried. The paper strength has mainly been determined by fibre *WRV* and fibre length. The reason that the fibre swells is because of the porous structure. This structure allows water to enter the pores and to affect the polar hydroxyl bonds connecting the cellulose or hemicellulose molecular chains. This causes the distance between the cellulose molecular chains to increase and hence the fibre to swell. In general, the fractal dimension reflects the structure characteristic of a pore material (Yang 2001). The more fine pores a material has, the rougher the surface: this leads to an increase in the value of *D*. In other words, the larger *D* is, the more the fibre surface pores there are, and hence water can more easily reach the cellulose surface, causing swelling. However, whether swelling occurs or not is finally determined by amount of the amorphous areas in the fibre and the amount of dissociative hydroxyl groups on the cellulose surface (Cao et al. 1998; Nazhad and Paszner 1994; Newman and Hemmingson 1997; Tze and Gardner 2001).

As shown in Table 3, with the increase in number of cycles, *WRV* and *D* fell. However, *WRV* decreased to 72.2% while *D* decreased to 97.7% after four cycles. This showed that *WRV* of the fibre was not only affected by its fractal dimension, but also by other factors, such as the crystallinity of cellulose (Chen et al. 2009).

CONCLUSIONS

This work presents an attempt to characterize the variation of pore structure in eucalyptus fibre during recycling. AFM survey showed that the pore structure in fibre expressed high self-similarity in statistical terms. Therefore the pore structure in fibre could be regard as a fractal. Fractal geometry analysis of the results showed that the fractal dimension of eucalyptus virgin fibre is 2.954. With increasing number of cycles, the fractal dimension decreased. WRV of the fibre was related not only to its fractal dimension, but also depended on the crystallinity of cellulose.

ACKNOWLEDGMENTS

This work was supported by a grant from by the National High Technology Research and Development Program of China (No. 2007AA03Z433) and the Natural Science Youth Fund Project of South China University of Technology. We thank the School of Environmental Science and Engineering, South China University of Technology, for the use of the micropore analyzer. We also thank State Key Laboratory of Pulp and Paper Engineering, South China University of Technology for the use of the Rapid-Köthen sheet former.

REFERENCES CITED

Andreasson, B., Forsstrom, J., and Wagberg, L. (2003). "The porous structure of pulp fibres with different yields and influence on paper strength," *Cellulose* 10,111-123.

Atzeni, C., Pia, G., Sanna, U., and Spanu, N. (2008). "A fractal model of the porous microstructure of earth-based materials," *Construction and Building Materials*, 22(8), 1607-1613.

Avnir, D., Farin, D., and Pfeifer, P. (1983). "Chemistry in noninteger dimensions between two and three. II. Fractal surfaces of adsorbents," *Journal of Chemical Physics*, 79(7), 3566-3571.

Böttger, J., Thi, L., and Krause, T. (1983). "Untersuchungen zur Porenstruktur von Zellstoffasern," *Das Papier*, 37(10A), 14-21.

Berthold, J., and Salmén, L. (1997). "Inverse size exclusion chromatography(ISEC) for determing the relative pore size distribution of wood pulps," *Holzforschung*, 51(4), 361-368.

Cao, B. J., Tschirner. U. and Ramaswamy, S. (1998). "Impact of pulp chemical composition on recycling," *Tappi Journal*, 81, 119-127.

Chen, Y. M., Wan, J. Q., Ma, Y. W. (2009). "Effect of noncellulosic constituents on physical properties and pore structure of recycled fibre," *APPITA Journal* 62(4), 290-295, 302.

Coppens, M. O., and Froment, G. F. (1995). "Knudsen diffusion in porous catalysts with a fractal internal surface," *Fractals* 3(4), 807-820.

Diniz, J. M. B. F., Gil, M. H. and Castro, J. A. A. M. (2004). "Hornification – Its origin and interpretation in wood pulps," *Wood Science Technology* 37, 489-494.

Dobrescu, G., Berger, D., Papa, F., and Ionescu, N. I. (2003). "Fractal dimensions of lanthanum ferrite samples by adsorption isotherm method," *Applied Surface Science*, 220(1-4), 154-158.

Fahlén, J., and Salmén, L. (2003). "Cross-sectional structure of the secondary wall of wood fibers as affected by processing," *Journal of Materials Science* 38,119-126.

Farin, D., and Avnir, D. (1988). "The fractal nature of molecule-surface chemical activities and physical interactions in porous materials," In: *Characterization of Porous Solids*, *Proceedings of the IUPAC Symposium (COPSI),*" Unger, K. K., Rouquerol, J., Sing, K. S. W., and Kral, H. (eds.), Elsevier, Amsterdam, 421-432.

Fernandes Diniz, J. M. B., Gil, M. H., and Castro, J. A. A. M. (2004). "Hornification – Its origin and interpretation in wood pulps," *Wood Sci. Technol*. 37, 489-494.

Forsström, J., Andreasson, B., and Wåqberg, L. (2005). "Influence of pore structure and water retaining ability of fibres on the strength of papers from unbleached kraft fibres," *Nordic Pulp & Paper Research Journal* 20 (2), 176-185.

Friesen, W. I., and Mikula, R. J. (1987). "Fractal dimensions of coal particles," *Journal of Colloid and Interface Science* 120(1), 263-271.

Gustafsson, J., Ciovica, L., and Peltonen, J. (2003). "The ultrastructure of spruce kraft pulps studied by atomic force microscopy (AFM) and X-ray photoelectron spectroscopy (XPS)," *Polymer* 44(3), 661-670.

Häggkvist, M., Li, T. Q., and Ödberg, L. (1998). "Effects of drying and pressing on the pore structure in the cellulose fibre wall studied by ^{1}H and ^{2}H NMR relaxation," *Cellulose* 5, 33-49 (1998).

Katz, A. J., and Thompson, A. H. (1985). "Fractal sandstone pores: Implications for conductivity and pore formation," *Physical Review Letters* 54(12), 1325-1328.

Kontturi, E., and Vuorinen, T. (2009). "Indirect evidence of supramolecular changes within cellulose microfibrils of chemical pulp fibers upon drying," *Cellulose* 16, 65-74.

Leon, C. A. L. Y. (1998). "New perspectives in mercury porosimetry," *Advances in Colloid and Interface Science* 76-77, 341-372.

Li, T. Q., and Eriksson, U. (1994). "Kaolin-based coating layer studied by 2H and 1H NMR relaxation method," *Langmuir* 10, 4624-4629.

Liu, D. J. (2006). *Fractal Theory Application in Chemical Engineering*, Chemical Industry Press, Beijing.

Maloney, T. C., and Paulapuro, H. (1999). "The formation of pores in the cell wall," *Journal of Pulp and Paper Science* 25(12), 430-436.

Mancosky, D. G., Lucia, L. A., and Deng, Y. L. (2004). "The effects of lignocellulosic fiber surface area on the dynamics of lignin oxidation and diffusion," *Journal of Applied Polymer Science* 94(1), 177-181.

Mandelbrot, B. B. (1982). *The Fractal Geometry of Nature*, Freeman, New York.

Nazhad, M. M., and Paszner, L. (1994). "Fundamentals of strength loss in recycled paper," *Tappi Journal* 77(9), 171-179.

Newman, R., and Hemmingson, J. (1997). "Cellulose cocrystallisation in hornification of kraft pulp," 9th ISWPC (pp.1-4). Montreal, Canada.

Notley, S. M., and Wågberg, L. (2005). "Morphology of modified regenerated model cellulose II surfaces studied by atomic force microscopy: Effect of carboxymethylation and heat treatment," *Biomacromolecules* 6(3),1586-1591.

Pitchumani, R., and Ramakrishnan, B. (1999). "A fractal geometry model for evaluating permeabilities of porous performs used in liquid composite molding," *International Journal Heat and Mass Transfer* 42(12), 2219-2232.

Pachulski, N., and Ulrich, J. (2007). "New fields of application for sol-gel process cold and vacuum-free 'compacting' of pharmaceutical materials to tablets," *Chemical Engineering Research & Design* 85(A7), 1013-1019.

Passe-Coutrin, N., Altenor, S., Cossement, D., Jean-Marius, C., and Gaspard, S. (2008). "Comparison of parameters calculated from the BET and Freundlich isotherms obtained by nitrogen adsorption on activated carbons: A new method for calculating the specific surface area," *Microporous and Mesoporous Materials* 111(1-3), 517-522.

Pfeifer, P., and Avnir, D. (1983). "Chemistry in noninteger dimensions between two and three. I. Fractal theory of heterogeneous surface," *Journal of Chemical Physics*, 79(7), 3558-3565.

Shao, S. Y. (2001). "Recycled properties of straw pulp," *Hubei Paper* 4, 11-14.

Sing, K. (2001). "The use of nitrogen adsorption for the characterisation of porous materials," *Colloids and Surfaces A: Physicochemical and Engineering Aspects*, 187(31), 3-9.

Stone, J. E. and Scallan, A. M. (1965). "Effects of component removal upon the porous structure of the cell wall of wood," *Journal of Polymer Science Part C: Polymer Symposia* 11(1), 13-25.

Topgaard, D., and Soderman, O. (2002). "Changes of cellulose fiber wall structure during drying investigated using NMR self diffusion and relaxation experiments," *Cellulose* 9,139-147.

Tze, W. T. and Gardner, D. J. (2001). "Contact angle and IGC measurements for probing surface-chemical changes in the recycling of wood pulp fibers," *Journal of Adhesion Science and Technology* 15(2), 223-241.

Wang, Y. L., Du, B. Y., Liu, J., Lu, J., Shi, B. Y. and Tang, H. X. (2007). "Surface analysis of cryofixation–vacuum –freeze-dried polyaluminum chloride–humic acid (PACl–HA) flocs," *Journal of Colloid and Interface Science* 316, 457-466.

Weise, U., and Paulapuro, H. (1996). "Relation between fiber shrinkage and hornification," *Papier*, 50 (6), 328-333.

Yang, S. H. (2001). "*Plant Fibre Chemistry"*, Chinese Light Industry Press, Beijing.

Yu, B. M. (2003). "Advances of fractal analysis of transport properties for porous media," *Advances in Mechanics* 33(3), 333-346.

Yu, C. T., Chen, W. H., Men, L. C. and Hwang, W. S. (2009). "Microscopic structure features changes of rice straw treated by boiled acid solution," *Industrial Crops and Products* 29, 308-315.

Article submitted: July 28, 2010; Peer review completed: February 11, 2011; Revised version received and accepted: February 14, 2011; Published: February 16, 2011.